Decoherence and entanglement evolution of two qubits coupled through Heisenberg interactions to a spin bath in thermal equilibrium

2007 J. Phys. A: Math. Theor. 40 11569

(http://iopscience.iop.org/1751-8121/40/38/009)

IOP Publishing Journal of Physics A: Mathematical and Theoretical

J. Phys. A: Math. Theor. **40** (2007) 11569–11591 doi:10.1088/1751-8113/40/38/009

Decoherence and entanglement evolution of two qubits coupled through Heisenberg interactions to a spin bath in thermal equilibrium

Y Hamdouni

School of Physics, University of KwaZulu-Natal, Westville Campus, Durban 4001, South Africa

E-mail: hamdouni@ukzn.ac.za

Received 31 May 2007, in final form 8 August 2007
Published 4 September 2007
Online at stacks.iop.org/JPhysA/40/11569

Abstract

The decoherence and entanglement dynamics of two interacting qubits coupled through Heisenberg XY interactions to a spin bath in thermal equilibrium are studied. The exact form of the reduced density matrix is derived for finite and infinite numbers of environmental spins. It is shown that decoherence can be minimized at low bath temperatures and strong coupling between the qubits. Some initial product states evolve into entangled ones, initially entangled states lose completely or partially their entanglement. The relation between the fidelity and the concurrence is also investigated.

PACS numbers: 03.65.Yz, 75.10.Jm, 03.67.Mn, 73.21.La

1. Introduction

Entanglement is the most intriguing feature of quantum mechanics. It is a nonlocal correlation between separate quantum-mechanical systems which does not have a classical counterpart. Besides its fundamental importance in the foundation of quantum mechanics [1–3], entanglement is considered as a valuable resource for quantum communications and information processing [4–9] since it helps speeding-up implementation of quantum algorithms and quantum communication protocols [10]. Considerable effort, both theoretically and experimentally, have been devoted to the understanding of entanglement. Recently, intense interest has been given to interacting spin systems which were proposed as candidates to achieve gate operations in solid-state quantum computation processors [11, 12]. This choice is motivated by the fact that such systems can be easily manipulated (e.g. by tunnelling potentials and energy bias), and scaled up to large registers. Hence, it is important to investigate entanglement generation and dynamics in spin systems.

On the other hand, quantum systems suffer decoherence because of their unwanted interactions with the surrounding environment. The decoherence process is indeed the major

obstacle for quantum information processing because it directly affects quantum interferences and correlations (entanglement) of quantum systems, leading them to behave classically [13–15]. Many strategies such as error-correcting codes and decoherence free subspaces were proposed in order to protect fragile quantum information against the detrimental effect of decoherence [16–22]. A number of theoretical studies have dealt with bosonic environments for which the Markovian approximation along with the master equation approach is often used. It turns out that the main contribution to decoherence in many solid-state systems (e.g. quantum dots) arises from the coupling to localized modes like nuclear spins, which can be effectively regarded as spin baths [23]. Recently, attention has been focused on the non-Markovian dynamics of multi-qubit systems interacting with spin environments [24–29]. In our earlier work [24], we have studied the reduced dynamics of the two-qubit system coupled through Heisenberg XY interactions to the spin star bath which was assumed at infinite temperature. We neglected the interaction between the central qubits. Later, Yuan *et al* [25] derived the dynamics of the two interacting qubits for particular initial states and finite bath temperature, using Holstein–Primakoff transformations expanded up to the first order with respect to the number of environmental spins. The elements of the resulting reduced density matrix were given in the thermodynamic limit by infinite series. In the following paper, we derive the exact dynamics of the central qubits, for an arbitrary number of environmental spins at finite bath temperature, without making recourse to any approximation. The key ingredient in this case consists of the underlying symmetries of the model Hamiltonian which facilitate the derivation of exact analytical results.

The paper is organized as follows. In section 2, we introduce the model Hamiltonian of the composite system qubits-bath. In section 3 after we derive the analytical form of the time evolution operator, we calculate the reduced density matrix for both finite and infinite number of spins in the environment. In section 4, we investigate decoherence and entanglement evolution of the two-qubit system for different initial states. A brief conclusion ends the paper.

2. The model

The system under consideration consists of a pair of interacting spin-$\frac{1}{2}$ particles (qubits) coupled to a quantum bath composed of a large number of spin-$\frac{1}{2}$ particles in thermal equilibrium at temperature T. The number of environmental spins is denoted by N. The Hamiltonian of the composite system is given by the sum of three operators, namely

$$H = H_0 + H_B + H_I. \tag{1}$$

H_0 describes the interaction between the central spins, it is given by the anisotropic Heisenberg Hamiltonian

$$H_0 = \Omega\left(\sigma_x^1\sigma_x^2 + \sigma_y^1\sigma_y^2\right) + \lambda\sigma_z^1\sigma_z^2, \tag{2}$$

where λ and Ω denote the strength of interactions, and σ_ν^i (with $\nu \equiv x, y, z$) is the ν-component of the pauli operator $\vec{\sigma}^i$ associated with qubit number i. The corresponding spin-flip operators are defined by $\sigma_\pm^i = \sigma_x^i \pm \sigma_y^i$.

Similarly, the environmental spins interact with each other through long-range anisotropic Heisenberg interactions. These are described by the bath Hamiltonian

$$H_B = \frac{g}{N}\sum_{i<j}^{N}\left(S_{Bx}^i S_{Bx}^j + S_{By}^i S_{By}^j + \Delta S_{Bz}^i S_{Bz}^j\right), \tag{3}$$

where $S_B^i (i = 1, 2, \ldots, N)$ are the spin operators of bath constituents, g is the strength of interactions and Δ is the anisotropy constant. The central spins couple to the environment through Heisenberg XY interactions; the corresponding Hamiltonian operator is given by

$$H_I = \frac{\alpha}{\sqrt{N}}\left[\left(\sigma_x^1 + \sigma_x^2\right)\sum_{i=1}^{N} S_{Bx}^i + \left(\sigma_y^1 + \sigma_y^2\right)\sum_{i=1}^{N} S_{By}^i\right]. \tag{4}$$

In the above equation α designates the coupling constant of the qubits to the bath. Note that the coupling constants g and α are rescaled by, respectively, N and $\sqrt{N}$ in order to ensure good thermodynamical behaviour.

By introducing the total spin operator of the environment, $\vec{J} = \frac{1}{2}\sum_{j=1}^{N}\vec{\sigma}^{\,j}$, together with the corresponding lowering and raising operators, $J_\pm = J_x \pm \mathrm{i}J_y$, it can be shown that (up to a trivial constant)

$$H_I + H_B = \frac{\alpha}{\sqrt{N}}\left[\left(\sigma_+^1 + \sigma_+^2\right)J_- + \left(\sigma_-^1 + \sigma_-^2\right)J_+\right] + \frac{g}{2N}\left[J^2 + (\Delta - 1)J_z^2\right]. \tag{5}$$

Clearly, the model Hamiltonian is invariant under rotations with respect to the z-direction. One can show by a direct calculation that the operator $J_z + S_z^1 + S_z^2$, where $S_z^i = \frac{1}{2}\sigma_z^i$, commutes with H, i.e. $[H,\, J_z + S_z^1 + S_z^2]_- = 0$. This simply implies that the z-component of the total spin of the composite system is conserved.

The spin space corresponding to the central system is given by $\mathbb{C}^2 \otimes \mathbb{C}^2 = \mathbb{C}^1 \oplus \mathbb{C}^3$. The subspace $\mathbb{C}^3$ is spanned by the state vectors $|1,-1\rangle$, $|1,0\rangle$ and $|1,1\rangle$. These are related to the basis vectors of $\mathbb{C}^2 \otimes \mathbb{C}^2$ (called computational basis vectors) by $|1,\pm 1\rangle = |\pm,\pm\rangle$ and $|1,0\rangle = \frac{1}{\sqrt{2}}(|-+\rangle + |+-\rangle)$. The space $\mathbb{C}^1$, in turn, is spanned by the antisymmetric maximally entangled bell state $|0,0\rangle = \frac{1}{\sqrt{2}}(|-+\rangle - |+-\rangle)$. The above equalities fully determine the unitary transformation that enables us to go from one basis to the other.

The standard basis of the bath space, $(\mathbb{C}^2)^{\otimes N}$, is composed of the joint eigenvectors of J^2 and J_z which we denote by $|j,m\rangle$, where $J^2|j,m\rangle = j(j+1)|j,m\rangle$ and $J_z|j,m\rangle = m|j,m\rangle$. Note that $0 \leqslant j \leqslant N/2$ and $-j \leqslant m \leqslant j$. One can then decompose the spin space of the environment as the direct sum of subspaces $\mathbb{C}^{d_j}$, each of which has dimension $d_j = 2j+1$, namely

$$(\mathbb{C}^2)^{\otimes N} = \bigoplus_{j=0}^{N/2} \nu(N,\, j)\mathbb{C}^{d_j}. \tag{6}$$

Here $\nu(N,\, j)$ is the multiplicity associated with j. In order to determine the explicit value of $\nu(N,\, j)$, let us introduce the subspace F_m of vectors $\vartheta \in (\mathbb{C}^2)^{\otimes N}$ satisfying $J_z\vartheta = m\vartheta$ [30]. The latter space can be decomposed as a direct sum of subspaces $E_{j,m}$ formed by the vectors $\bar{\vartheta}$ for which $J^2\bar{\vartheta} = j(j+1)\bar{\vartheta}$. Thus, we simply have $F_m = \bigoplus_{j=m}^{N/2} E_{j,m}$ and $\dim(F_m) = \sum_{j=m}^{N/2}\dim(E_{j,m}) = \binom{N}{\frac{N}{2}-m}$. From the above, it immediately follows that

$$\nu(N,\, j) = \dim(F_j) - \dim(F_{j+1}) = \binom{N}{\frac{N}{2}-j} - \binom{N}{\frac{N}{2}-j-1}. \tag{7}$$

3. Exact time evolution

This section deals with the derivation of the exact reduced dynamics of the central qubits. The time dependence of the total density matrix describing the state of the composite system is given as usual by

$$\rho_{\mathrm{tot}}(t) = \mathbf{U}(t)\rho_{\mathrm{tot}}(0)\mathbf{U}^\dagger(t), \tag{8}$$

where $\mathbf{U}(t) = \exp(-\mathrm{i}Ht)$ is the time evolution operator and $\rho_{\mathrm{tot}}(0)$ is the initial total density matrix. In the following, after we introduce the initial states of the central system and the bath,

we derive the exact analytical form of $\mathbf{U}(t)$, then we calculate the time-dependent reduced density matrix $\rho(t)$ for both finite and infinite number of environmental spins.

3.1. Initial conditions

At $t = 0$ the central two-qubit system is assumed to be decoupled from the environment. This means that $\rho_{\text{tot}}(0)$ factorizes into the following direct product:

$$\rho_{\text{tot}}(0) = \rho(0) \otimes \rho_B(0), \tag{9}$$

where $\rho(0)$ and $\rho_B(0)$ are, respectively, the initial density matrices corresponding to the two-qubit system and the environment.

Initially, the spin environment is taken in thermal equilibrium at the finite temperature T. The density matrix $\rho_B(0)$ is simply given by the Boltzmann distribution

$$\rho_B(0) = \frac{1}{Z_N} \mathrm{e}^{-\frac{g\beta}{2N}[J^2+(\Delta-1)J_z^2]}, \tag{10}$$

where $Z_N = \mathrm{tr}_B\left\{\mathrm{e}^{-\frac{g\beta}{2N}[J^2+(\Delta-1)J_z^2]}\right\}$ is the partition function corresponding to the spin bath and $\beta = \frac{1}{T}$ is the inverse temperature. Note that the Boltzmann constant is set to one, i.e. $k_B = 1$. The partition function Z_N can be expressed as [31]

$$Z_N = \sum_{j=0}^{N/2} \nu(N, j) \sum_{m=-j}^{j} \mathrm{e}^{-\frac{g\beta}{2N}[j(j+1)+(\Delta-1)m^2]}. \tag{11}$$

In particular, we have $\lim_{\beta\to 0} \rho_B(0) = 2^{-N}\mathbb{I}_N$, where $\mathbb{I}_N$ stands for the unity matrix in the bath space.

Let us now assume that at $t = 0$ the two-qubit system is prepared in the normalized state $|\Psi(0)\rangle = \sum_i a_i|\xi_i\rangle$, where $|\xi_i\rangle \in \{|1,-1\rangle, |1,0\rangle, |1,1\rangle, |0,0\rangle\}$ and $\sum_i |a_i|^2 = 1$. Therefore, the initial density matrix of the central spins can be written in the standard basis of $\mathbb{C}^1 \oplus \mathbb{C}^3$ as

$$\rho(0) = \sum_{ij} \rho_{ij}^0 |\xi_i\rangle\langle\xi_j|, \qquad \rho_{ij}^0 = a_i a_j^*, \sum_{i=1}^{4} \rho_{ii}^0 = 1. \tag{12}$$

The time-dependent density matrix $\rho(t)$ is calculated by performing the trace with respect to the environmental degrees of freedom, i.e. $\rho(t) = \mathrm{tr}_B\{\rho_{\text{tot}}(t)\}$. This can be rewritten in terms of the common eigenvectors of J^2 and J_z as follows:

$$\rho(t) = \sum_{k,\ell} \rho_k^0 \sum_{j=0}^{N/2} \nu(N, j) \sum_{m=-j}^{j} \langle jm|\mathbf{U}(t)|\xi_k\rangle \rho_B(0) \langle\xi_\ell|\mathbf{U}^\dagger(t)|jm\rangle. \tag{13}$$

3.2. Time evolution operator

Before we proceed with the determination of the reduced dynamics, it should be noted that the evolution in time of the central qubits depends on the nature of interactions between the spins in the environment. In the case of single central spin it is found that for antiferromagnetic interactions within the bath, the effect of the anisotropy constant Δ can be neglected when the number of environmental spins becomes sufficiently large (typically of the order of 100) [29]. The above result is independent of the number of central qubits as long as their coupling to the bath does not include interactions of the form $\sigma_z^i \otimes J_z$. Hence, it is sufficient to investigate the isotropic case which exhibits the advantage of making our model exactly solvable. This

is mainly due to the fact that $[H_B, H_I] = 0$ when $\Delta = 1$, implying that the time evolution operator reduces to $\exp\{-\mathrm{i}(H_0 + H_I)\}$.

It is worth mentioning that due to symmetry, states belonging to $\mathbb{C}^3$ and $\mathbb{C}^1$ never mix; they evolve independently from each other without leaving the subspaces to which they belong. Thus we can write the model Hamiltonian as the direct sum of two operators living in the above subspaces. Indeed, the Hamiltonian operators H_0 and H_I can be written in $\mathbb{C}^3 \otimes (\mathbb{C}^2)^{\otimes N}$ (up to a trivial constant for H_0) as

$$H_0 = \begin{pmatrix} \epsilon & 0 & 0 \\ 0 & -\epsilon & 0 \\ 0 & 0 & \epsilon \end{pmatrix} \otimes \mathbb{I}_N, \qquad H_I = \frac{\alpha}{\sqrt{N}} \begin{pmatrix} 0 & J_+ & 0 \\ J_- & 0 & J_+ \\ 0 & J_- & 0 \end{pmatrix}, \tag{14}$$

where $\epsilon = \lambda - \Omega$. Similarly, in the subspace $\mathbb{C}^1 \otimes (\mathbb{C}^2)^{\otimes N}$ we can rewrite the free Hamiltonian as $H_0 = -\kappa \mathbb{I}_N$, where $\kappa = 3\Omega + \lambda$. Since the action of the interaction Hamiltonian vanishes in this subspace, it immediately follows that $H^n = (-\kappa)^n$. Furthermore, it can be shown that in $\mathbb{C}^3 \otimes (\mathbb{C}^2)^{\otimes N}$ the operator H_0 anticommutes with H_I, i.e. $[H_0, H_I]_+ = 0$ and $H^2 = H_I^2 + \epsilon^2$. We have shown in [24] that in $\mathbb{C}^3 \otimes (\mathbb{C}^2)^{\otimes N}$, the powers of H_I are given by

$$H_I^{2n} = \left(\frac{\alpha}{\sqrt{N}}\right)^{2n} \begin{pmatrix} J_+ K^{n-1} J_- & 0 & J_+ K^{n-1} J_+ \\ 0 & K^n & 0 \\ J_- K^{n-1} J_- & 0 & J_- K^{n-1} J_+ \end{pmatrix}, \tag{15}$$

$$H_I^{2n+1} = \left(\frac{\alpha}{\sqrt{N}}\right)^{2n+1} \begin{pmatrix} 0 & J_+ K^n & 0 \\ K^n J_- & 0 & K^n J_+ \\ 0 & J_- K^n & 0 \end{pmatrix}, \tag{16}$$

where $K = J_+ J_- + J_- J_+ = 2\big(J^2 - J_z^2\big)$. Using the above relations it is possible to derive general expressions for even and odd powers of $H = H_0 + H_I$.

As an example, let us calculate H_{11}^{2n}. We have for $n \geqslant 1$

$$H^{2n} = \sum_{k=0}^{n} H_I^{2k} \epsilon^{2(n-k)} \binom{n}{k}. \tag{17}$$

Therefore,

$$H_{11}^{2n} = \epsilon^{2n} + J_+ \sum_{\ell=1}^{n} \tilde{\alpha}^{2\ell} K^{\ell-1} \epsilon^{2(n-\ell)} \binom{n}{\ell} J_- = \epsilon^{2n} \tag{18}$$

$$+ J_+ \sum_{\ell=0}^{n} \left[\frac{\tilde{\alpha}^{2\ell}}{K} K^{\ell} \epsilon^{2(n-\ell)} \binom{n}{\ell} - \frac{\epsilon^{2n}}{K} \right] J_- = \epsilon^{2n} + J_+ \frac{(\epsilon^2 + \tilde{\alpha}^2 K)^n - \epsilon^{2n}}{K} J_-, \tag{19}$$

where we have introduced $\tilde{\alpha} = \alpha/\sqrt{N}$ for the ease of notation. Using the same method we get

$$H^{2n} = \begin{pmatrix} \epsilon^{2n} + J_+ \frac{(\epsilon^2+\tilde{\alpha}^2 K)^n - \epsilon^{2n}}{K} J_- & 0 & J_+ \frac{(\epsilon^2+\tilde{\alpha}^2 K)^n - \epsilon^{2n}}{K} J_+ \\ 0 & (\epsilon^2 + \tilde{\alpha}^2 K)^n & 0 \\ J_- \frac{(\epsilon^2+\tilde{\alpha}^2 K)^n - \epsilon^{2n}}{K} J_- & 0 & \epsilon^{2n} + J_- \frac{(\epsilon^2+\tilde{\alpha}^2 K)^n - \epsilon^{2n}}{K} J_+ \end{pmatrix}, \tag{20}$$

$$H^{2n+1} = \begin{pmatrix} \epsilon^{2n+1} + \epsilon J_+ \frac{(\epsilon^2+\tilde{\alpha}^2 K)^n - \epsilon^{2n}}{K} J_- & \tilde{\alpha} J_+ (\epsilon^2 + \tilde{\alpha}^2 K)^n & \epsilon J_+ \frac{(\epsilon^2+\tilde{\alpha}^2 K)^n - \epsilon^{2n}}{K} J_+ \\ \tilde{\alpha}(\epsilon^2 + \tilde{\alpha} K)^n J_- & -\epsilon(\epsilon^2 + \tilde{\alpha}^2 K)^n & \tilde{\alpha}(\epsilon^2 + \tilde{\alpha}^2 K)^n J_+ \\ \epsilon J_- \frac{(\epsilon^2+\tilde{\alpha}^2 K)^n - \epsilon^{2n}}{K} J_- & \tilde{\alpha} J_- (\epsilon^2 + \tilde{\alpha}^2 K)^n & \epsilon^{2n+1} + \epsilon J_- \frac{(\epsilon^2+\tilde{\alpha}^2 K)^n - \epsilon^{2n}}{K} J_+ \end{pmatrix}. \tag{21}$$

Now we have all the ingredients that enable us to derive the explicit form of the time evolution operator. Indeed, expanding $\mathbf{U}(t)$ in Tailor series and using equations (20) and (21) we find that the matrix elements of the time evolution operator in the space $\mathbb{C}^3 \oplus \mathbb{C}^1$ are given by ($\hbar = 1$)

$$U_{11}(t) = \exp(-\mathrm{i}\epsilon t) + J_+\left[\frac{\cos(tM) - \cos(\epsilon t)}{K} - \mathrm{i}\frac{\epsilon\sin(tM) - M\sin(\epsilon t)}{KM}\right]J_-, \tag{22}$$

$$U_{12}(t) = -\mathrm{i}\tilde{\alpha}J_+\frac{\sin(tM)}{M}, \tag{23}$$

$$U_{13}(t) = J_+\left[\frac{\cos(tM) - \cos(\epsilon t)}{K} - \mathrm{i}\frac{\epsilon\sin(tM) - M\sin(\epsilon t)}{KM}\right]J_+, \tag{24}$$

$$U_{22}(t) = \cos(tM) + \mathrm{i}\epsilon\frac{\sin(tM)}{M}, \tag{25}$$

$$U_{23}(t) = -\mathrm{i}\tilde{\alpha}\frac{\sin(tM)}{M}J_+, \tag{26}$$

$$U_{33}(t) = \exp(-\mathrm{i}\epsilon t) + J_-\left[\frac{\cos(tM) - \cos(\epsilon t)}{K} - \mathrm{i}\frac{\epsilon\sin(tM) - M\sin(\epsilon t)}{KM}\right]J_+, \tag{27}$$

$$U_{14}(t) = U_{24}(t) = U_{34}(t) = 0, \tag{28}$$

$$U_{44}(t) = \exp(\mathrm{i}\kappa t), \tag{29}$$

where we have introduced the operator $M = \sqrt{\epsilon^2 + \alpha^2 K/N}$. The remaining matrix elements can be found by simply taking the transpose (not the Hermitian conjugate) of those listed above. Taking into account the trace properties of the lowering and raising operators, it can be shown by virtue of equation (13) that the elements of the reduced density matrix can be written as

$$\rho_{11}(t) = \mathrm{tr}_B\left\{\rho_B(0)\left[\rho^0_{11}U_{11}(t)U^\dagger_{11}(t) + \rho^0_{22}U_{12}(t)U^\dagger_{12}(t) + \rho^0_{33}U_{13}(t)U^\dagger_{13}(t)\right]\right\} \tag{30}$$

$$\rho_{12}(t) = \mathrm{tr}_B\left\{\rho_B(0)\left[\rho^0_{12}U_{11}(t)U^\dagger_{22}(t) + \rho^0_{23}U_{12}(t)U^\dagger_{23}(t)\right]\right\} \tag{31}$$

$$\rho_{13}(t) = \mathrm{tr}_B\left\{\rho_B(0)\left[\rho^0_{13}U_{11}(t)U^\dagger_{33}(t)\right]\right\} \tag{32}$$

$$\rho_{14}(t) = \mathrm{tr}_B\left\{\rho_B(0)\left[\rho^0_{14}U_{11}(t)U^\dagger_{44}(t)\right]\right\} \tag{33}$$

$$\rho_{22}(t) = \mathrm{tr}_B\left\{\rho_B(0)\left[\rho^0_{11}U_{21}(t)U^\dagger_{21}(t) + \rho^0_{22}U_{22}(t)U^\dagger_{22}(t) + \rho^0_{33}U_{23}(t)U^\dagger_{23}(t)\right]\right\} \tag{34}$$

$$\rho_{23}(t) = \mathrm{tr}_B\left\{\rho_B(0)\left[\rho^0_{12}U_{21}(t)U^\dagger_{32}(t) + \rho^0_{23}U_{22}(t)U^\dagger_{33}(t)\right]\right\} \tag{35}$$

$$\rho_{24}(t) = \mathrm{tr}_B\left\{\rho_B(0)\left[\rho^0_{24}U_{22}(t)U^\dagger_{44}(t)\right]\right\} \tag{36}$$

$$\rho_{33}(t) = \mathrm{tr}_B\left\{\rho_B(0)\left[\rho^0_{11}U_{31}(t)U^\dagger_{31}(t) + \rho^0_{22}U_{32}(t)U^\dagger_{32}(t) + \rho^0_{33}U_{33}(t)U^\dagger_{33}(t)\right]\right\} \tag{37}$$

$$\rho_{34}(t) = \mathrm{tr}_B\left\{\rho_B(0)\left[\rho^0_{34}U_{33}(t)U^\dagger_{44}(t)\right]\right\} \tag{38}$$

$$\rho_{44}(t) = \rho^0_{44}. \tag{39}$$

The remaining matrix elements are obtained by taking the complex conjugate of those listed above.

Figure 1 illustrates the time dependence of some elements of the reduced density matrix for different values of the number of spins in the environment. We can see that the curves

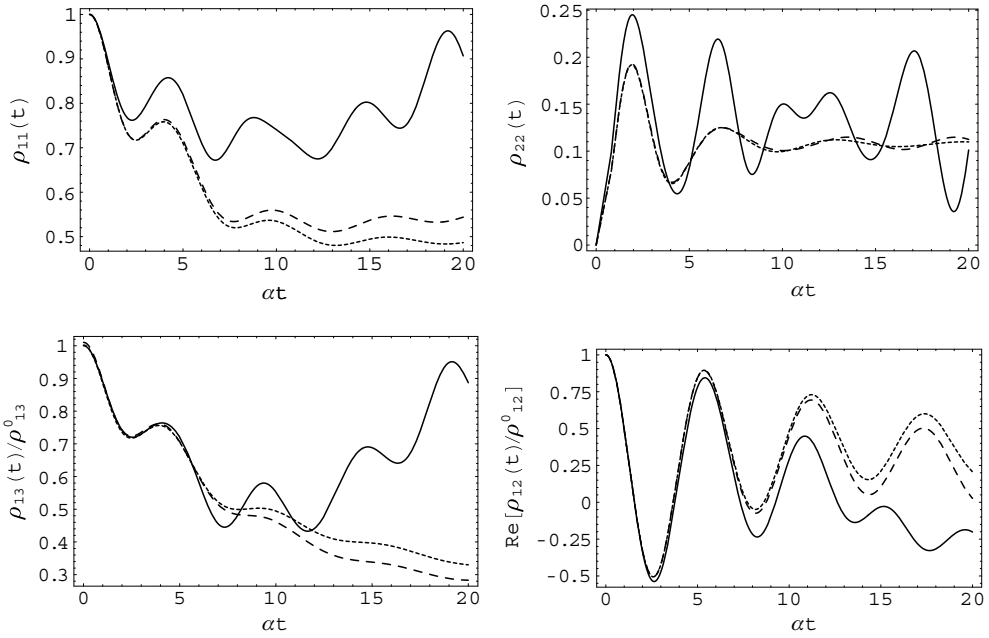

Figure 1. Evolution in time of some elements of the reduced density matrix for different values of environmental spins: $N = 10$ (solid lines), $N = 100$ (dashed lines) and $N = 300$ (dotted lines). The initial state corresponding to $\rho_{11}(t)$ and $\rho_{22}(t)$ is the product state $|- -\rangle$. Here we have set $\rho^0_{12} = \rho^0_{23}$. The parameters are $\epsilon = \alpha$ and $g\beta = 10$.

corresponding to each matrix element get more and more closer from each other as the number of bath spins increases. If we let N take sufficiently large values ($N \sim 100$), then the curves saturate with respect to N and become almost identical. In the following subsection we study the case in which $N \to \infty$. All the results regarding decoherence and entanglement evolution will be studied in this limit.

3.3. Infinite number of spins in the bath

In order to study the limit of an infinite number of environmental spins it should be stressed that the operators $J_\pm$ as well as J_z are traceless in the standard basis formed by the common eigenvectors of J^2 and J_z. Moreover, the scaled lowering and raising operators $J_\pm/\sqrt{N}$ are well-behaved fluctuation operators with respect to the tracial state on the bath, and satisfy

$$\lim_{N\to\infty} 2^{-N}\mathrm{tr}_B\left\{\prod_{i=1}^{k}\left(\frac{J_+J_-}{N}\right)^{n_i}\right\} = \frac{n!}{2^n}, \tag{40}$$

where $n = \sum_{i=1}^{k} n_i$ and $n_i \in \mathbb{N}$. This follows from the fact that [24, 27]

$$\mathrm{tr}_B\{(J_+J_-)^n\} \approx \frac{2^N N^n n!}{2^n}. \tag{41}$$

Thus , $J_+/\sqrt{N}$ converges to a normal complex random variable, z, with the probability density function [24]

$$z \mapsto \frac{2}{\pi}\,\mathrm{e}^{-2|z|^2}. \tag{42}$$

In particular, we can infer that

$$\lim_{N\to\infty} 2^{-N}\mathrm{tr}_B\left\{f\left(\frac{J_\pm J_\mp}{N}\right)\right\} = \frac{2}{\pi}\int_{\mathbb{C}} f(|z|^2)\,\mathrm{e}^{-2|z|^2}\,\mathrm{d}z\,\mathrm{d}z^* \tag{43}$$

provided that $|f(z)|$ does not increase faster than $\mathrm{e}^{-2|z|^2}$ for all $z \in \mathbb{C}$. This is typically the case for the functions $\mathrm{e}^{-ar^2}h(r^2)$ where $|h(r^2)| < \infty, r \in \mathbb{R}$ and $\mathrm{Re}(a) \geqslant -2$. Similarly, the operator $J_z/\sqrt{N}$ converges to a normal real random variable, τ, with the probability density function

$$\tau \mapsto \sqrt{\frac{2}{\pi}}\,\mathrm{e}^{-2\tau^2}. \tag{44}$$

In this case, a similar equation to (43) can be obtained by replacing $J_\pm/\sqrt{N}$ and $|z|$ by $J_z/\sqrt{N}$ and τ, respectively. We have already mentioned that for antiferromagnetic interactions within the bath, isotropic and anisotropic Heisenberg Hamiltonian operators with $\Delta \geqslant 0$ are completely equivalent when $N \to \infty$. Let us explain this a little bit. One can see that $\rho_B(0)$ always appears between two matrix elements of $\mathbf{U}(t)$. If we exchange the order of $\rho_B(0)$ with one of the above matrix elements, which is possible using simple commutation relations, we end up with extra operators of the form J_z/N. These can be indeed neglected when $N \to \infty$. Then using the cyclic property of the trace, it is possible to transform any function $\Upsilon_{ijk\ell} = U_{ij}U^\dagger_{k\ell}$ inside the trace sign into a function which depends on $\frac{J_\pm J_\mp}{N}$. Hence, for all $\Delta \geqslant 0$

$$\begin{aligned}\langle\Upsilon_{ijk\ell}\rangle &= \lim_{N\to\infty}\frac{1}{\mathrm{tr}_B\left\{\mathrm{e}^{\frac{-g\beta}{2N}[J^2+(\Delta-1)J_z^2]}\right\}}\mathrm{tr}_B\left\{\mathrm{e}^{\frac{-g\beta}{2N}[J^2+(\Delta-1)J_z^2]}\Upsilon_{ijk\ell}\left(\frac{J_\pm J_\mp}{N}\right)\right\}\\ &= \frac{\int_{\mathbb{R}}\int_{\mathbb{C}}\exp\{-(2+g\beta/2)|z|^2-(2+g\beta\Delta/2)\tau^2\}\Upsilon_{ijk\ell}(|z|^2)\,\mathrm{d}\tau\,\mathrm{d}z\,\mathrm{d}z^*}{\int_{\mathbb{R}}\int_{\mathbb{C}}\exp\{-(2+g\beta/2)|z|^2-(2+g\beta\Delta/2)\tau^2\}\,\mathrm{d}\tau\,\mathrm{d}z\,\mathrm{d}z^*}\\ &= \frac{\int_0^\infty \mathrm{e}^{-(2+g\beta/2)r^2}\Upsilon_{ijk\ell}(r^2)r\,\mathrm{d}r}{\int_0^\infty \mathrm{e}^{-(2+g\beta/2)r^2}r\,\mathrm{d}r} = (4+g\beta)\int_0^\infty \mathrm{e}^{-(2+g\beta/2)r^2}\Upsilon_{ijk\ell}(r^2)r\,\mathrm{d}r,\end{aligned} \tag{45}$$

where we have used polar coordinates (r,ϕ) to simplify the integrals with respect to the complex variable $z = r\mathrm{e}^{\mathrm{i}\phi}$. Clearly, the latter expression is independent of Δ. Using the above result we find that

$$\begin{aligned}\left\langle U_{11}U_{11}^\dagger\right\rangle &= \left\langle U_{11}U_{33}^\dagger\right\rangle = \left\langle U_{33}U_{33}^\dagger\right\rangle\\ &= \tfrac{1}{4}\left[\tfrac{3}{2}+\tfrac{1}{2}f(2t)+2\cos(\epsilon t)f(t)+g(t)+2\sin(\epsilon t)\ell(t)\right],\end{aligned} \tag{46}$$

$$\left\langle U_{12}U_{12}^\dagger\right\rangle = \left\langle U_{12}U_{23}^\dagger\right\rangle = \left\langle U_{23}U_{23}^\dagger\right\rangle = \left\langle U_{32}U_{32}^\dagger\right\rangle = h(t), \tag{47}$$

$$\left\langle U_{13}U_{13}^\dagger\right\rangle = \tfrac{1}{4}\left[\tfrac{3}{2}+\tfrac{1}{2}f(2t)-2\cos(\epsilon t)f(t)+g(t)-2\sin(\epsilon t)\ell(t)\right], \tag{48}$$

$$\left\langle U_{11}U_{22}^\dagger\right\rangle = \tfrac{1}{2}\left[\tfrac{1}{2}+\tfrac{1}{2}f(2t)-g(t)-\mathrm{i}\ell(2t)+\mathrm{e}^{-\mathrm{i}\epsilon t}(f(t)-\mathrm{i}\ell(t))\right], \tag{49}$$

$$\left\langle U_{22}U_{22}^\dagger\right\rangle = \tfrac{1}{2}[1+f(2t)+2g(t)], \tag{50}$$

$$\left\langle U_{22}U_{33}^\dagger\right\rangle = \tfrac{1}{2}\left[\tfrac{1}{2}+\tfrac{1}{2}f(2t)-g(t)+\mathrm{i}\ell(2t)+\mathrm{e}^{\mathrm{i}\epsilon t}(f(t)+\mathrm{i}\ell(t))\right], \tag{51}$$

$$\langle U_{11}\rangle = \langle U_{33}\rangle = \tfrac{1}{2}\left[f(t)-\mathrm{i}\ell(t)+\mathrm{e}^{-\mathrm{i}\epsilon t}\right], \tag{52}$$

$$\langle U_{22}\rangle = f(t)+\mathrm{i}\ell(t). \tag{53}$$

Here we have introduced the functions

$$\begin{aligned} f(t) &= \langle \cos(t\sqrt{\epsilon^2+2r^2})\rangle, & g(t) &= \left\langle \epsilon^2 \frac{\sin^2(t\sqrt{\epsilon^2+2r^2})}{\epsilon^2+2r^2}\right\rangle, \\ h(t) &= \left\langle r^2 \frac{\sin^2(t\sqrt{\epsilon^2+2r^2})}{\epsilon^2+2r^2}\right\rangle, & \ell(t) &= \left\langle \epsilon \frac{\sin(t\sqrt{\epsilon^2+2r^2})}{\sqrt{\epsilon^2+2r^2}}\right\rangle, \end{aligned} \tag{54}$$

where ϵ and t are, respectively, given in units of α^{-1} and α. Let us derive, for example, the explicit expression of $\ell(t)$. We have

$$\begin{aligned} \ell(t) &= \epsilon(4+g\beta)\int_0^\infty \mathrm{e}^{-(2+g\beta/2)r^2}\frac{\sin(t\sqrt{\epsilon^2+2r^2})}{\sqrt{\epsilon^2+2r^2}} r\,\mathrm{d}r \\ &= \frac{\epsilon}{2}(4+g\beta)\,\mathrm{e}^{\frac{\epsilon^2}{4}(4+g\beta)}\int_\epsilon^\infty \mathrm{d}\eta\,\mathrm{e}^{-\frac{\eta^2}{4}(4+g\beta)}\sin(\eta t), \end{aligned} \tag{55}$$

where we have made the change of variable $\eta^2 = \epsilon^2 + 2r^2$. The above expression can be further simplified to

$$\ell(t) = \epsilon\sqrt{4+g\beta}\exp\left[\frac{\epsilon^2}{4}(4+g\beta) - \frac{t^2}{4+g\beta}\right]\mathrm{Im}\left\{\int_a^\infty \mathrm{e}^{-\delta^2}\mathrm{d}\delta\right\}, \tag{56}$$

where $\delta = \frac{\eta}{2}\sqrt{4+g\beta} - \mathrm{i}\frac{t}{\sqrt{4+g\beta}}$, $a = \frac{\epsilon}{2}\sqrt{4+g\beta} - \mathrm{i}\frac{t}{\sqrt{4+g\beta}}$ and $\mathrm{Im}(x)$ stands for the imaginary part of x. The latter integral is nothing but the complementary error function [32], which can be transformed into a sum of two ordinary error functions and we simply get

$$\begin{aligned} \ell(t) = \frac{\mathrm{i}\sqrt{\pi}\epsilon}{4}\sqrt{4+g\beta}\exp\left[\frac{\epsilon^2}{4}(4+g\beta) - \frac{t^2}{4+g\beta}\right] \\ \times\left\{\mathrm{erf}\left[\frac{\epsilon/2(4+g\beta)-\mathrm{i}t}{\sqrt{4+g\beta}}\right] - \mathrm{erf}\left[\frac{\epsilon/2(4+g\beta)+\mathrm{i}t}{\sqrt{4+g\beta}}\right]\right\}, \end{aligned} \tag{57}$$

with

$$\mathrm{erf}(z) = \frac{2}{\sqrt{\pi}}\int_0^z \mathrm{e}^{-t^2}\,\mathrm{d}t. \tag{58}$$

Following the same method we find that

$$\begin{aligned} f(t) = \cos(\epsilon t) + \frac{\mathrm{i}t}{2}\sqrt{\frac{\pi}{4+g\beta}}\exp\left[\frac{\epsilon^2}{4}(4+g\beta) - \frac{t^2}{4+g\beta}\right] \\ \times\left\{\mathrm{erf}\left[\frac{\epsilon/2(4+g\beta)+\mathrm{i}t}{\sqrt{4+g\beta}}\right] - \mathrm{erf}\left[\frac{\epsilon/2(4+g\beta)-\mathrm{i}t}{\sqrt{4+g\beta}}\right]\right\}, \end{aligned} \tag{59}$$

$$\begin{aligned} g(t) = \frac{\epsilon^2(4+g\beta)}{8}\,\mathrm{e}^{\frac{\epsilon^2}{4}(4+g\beta)}\Gamma\left[0, \frac{\epsilon^2}{4}(4+g\beta)\right] - \frac{\epsilon^2(4+g\beta)}{4}\,\mathrm{e}^{\frac{\epsilon^2}{4}(4+g\beta)} \\ \times\int_\epsilon^\infty \mathrm{d}r\frac{\cos(2rt)}{r}\,\mathrm{e}^{-\frac{r^2}{4}(4+g\beta)}, \end{aligned} \tag{60}$$

$$\begin{aligned} h(t) = \frac{1}{4} - \frac{\epsilon^2}{16}(4+g\beta)\,\mathrm{e}^{\frac{\epsilon^2}{4}(4+g\beta)}\Gamma\left[0, \frac{\epsilon^2}{4}(4+g\beta)\right] - \frac{1}{4}\cos(2\epsilon t) \\ + \frac{\mathrm{i}t}{4}\sqrt{\frac{\pi}{4+g\beta}}\exp\left[\frac{\epsilon^2}{4}(4+g\beta) - \frac{4t^2}{4+g\beta}\right]\left\{\mathrm{erf}\left[\frac{\epsilon/2(4+g\beta)-2\mathrm{i}t}{\sqrt{4+g\beta}}\right]\right. \\ \left. - \mathrm{erf}\left[\frac{\epsilon/2(4+g\beta)+2\mathrm{i}t}{\sqrt{4+g\beta}}\right]\right\} + \frac{\epsilon^2(4+g\beta)}{8}\,\mathrm{e}^{\frac{\epsilon^2}{4}(4+g\beta)}\int_\epsilon^\infty \mathrm{d}r\frac{\cos(2rt)}{r}\,\mathrm{e}^{-\frac{r^2}{4}(4+g\beta)}, \end{aligned} \tag{61}$$

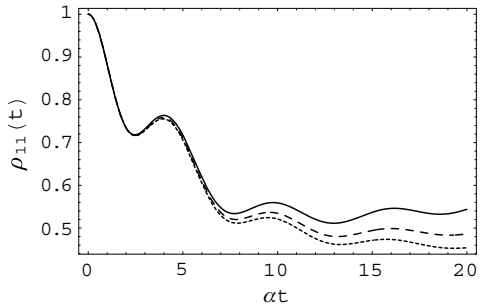

Figure 2. Comparison between the behaviour of $\rho_{11}(t)$ obtained for finite and infinite number of environmental spins: $N = 100$ (solid line), $N = 300$ (dashed line) and $N \to \infty$ (dotted line). The initial state is $|- -\rangle$ with $\epsilon = \alpha$ and $g\beta = 10$.

where

$$\Gamma(a, z) = \int_z^\infty t^{a-1}\, \mathrm{e}^{-t}\, \mathrm{d}t \tag{62}$$

is the incomplete gamma function. Note that the integral in equations (60) and (61) cannot be calculated analytically; we leave it in that form.

Using the Riemann–Lebesgue lemma it is possible to find the asymptotic behaviour (i.e. when $t \to \infty$) of the above functions, namely

$$f(\infty) = \ell(\infty) = 0, \tag{63}$$

$$g(\infty) = \frac{\epsilon^2}{8}(4 + g\beta)\, \mathrm{e}^{\frac{\epsilon^2}{4}(4+g\beta)}\Gamma\left[0, \frac{\epsilon^2}{4}(4 + g\beta)\right], \tag{64}$$

$$h(\infty) = \frac{1}{4} - \frac{\epsilon^2}{16}(4 + g\beta)\, \mathrm{e}^{\frac{\epsilon^2}{4}(4+g\beta)}\Gamma\left[0, \frac{\epsilon^2}{4}(4 + g\beta)\right]. \tag{65}$$

Furthermore, we can prove using the following asymptotic expression of the incomplete gamma function [32]

$$\Gamma(a, z) \sim z^{a-1}\, \mathrm{e}^{-z}\left[1 + \frac{a-1}{z} + \frac{(a-1)(a-2)}{z^2} + \cdots\right], \tag{66}$$

when $z \to \infty$ provided $|\arg z| < 3\pi/2$ that

$$\lim_{\beta,\epsilon\to\infty} g(\infty) = \tfrac{1}{2}, \qquad \lim_{\beta,\epsilon\to\infty} h(\infty) = 0. \tag{67}$$

The latter results will be used below to study decoherence and entanglement of the central qubits. In figure 2, we have displayed the evolution in time of $\rho_{11}(t)$ corresponding to the state $|- -\rangle$ for different vales of N including the limit $N \to \infty$.

3.4. Second-order master equation

The second-order master equation can be derived in the interaction picture by noting that

$$\tilde{\rho}_{\mathrm{tot}}(t) = \rho(0) \otimes \rho_B(0) - \mathrm{i}\int_0^t \mathrm{d}s[\tilde{H}_I(s), \tilde{\rho}_{\mathrm{tot}}(s)], \tag{68}$$

where $\tilde{A}(t) = \mathrm{e}^{\mathrm{i}H_0 t} A(t)\, \mathrm{e}^{-\mathrm{i}H_0 t}$. It is easy to see that

$$\mathrm{tr}_B\{[\tilde{H}_I(t), \rho(0) \otimes \rho_B(0)]\} = 0. \tag{69}$$

Then under Born approximation, one can show that the second-order master equation yields the following set of integro-differential equations:

$$\dot{\tilde{\rho}}_{11}(t) = -2\alpha^2 R \int_0^t \cos[2\epsilon(t-s)][\tilde{\rho}_{11}(s) - \tilde{\rho}_{22}(s)]\,\mathrm{d}s, \tag{70}$$

$$\dot{\tilde{\rho}}_{12}(t) = -\alpha^2 R\,\mathrm{e}^{2\mathrm{i}\epsilon t} \int_0^t [3\tilde{\rho}_{12}(s) - 2\tilde{\rho}_{23}(s)]\,\mathrm{d}s, \tag{71}$$

$$\dot{\tilde{\rho}}_{13}(t) = -2\alpha^2 R \int_0^t \cos[2\epsilon(t-s)]\tilde{\rho}_{13}(s)\,\mathrm{d}s, \tag{72}$$

$$\dot{\tilde{\rho}}_{22}(t) = -2\alpha^2 R \int_0^t \cos[2\epsilon(t-s)][2\tilde{\rho}_{22}(s) - \tilde{\rho}_{11}(s) - \tilde{\rho}_{33}(s)]\,\mathrm{d}s, \tag{73}$$

$$\dot{\tilde{\rho}}_{23}(t) = -\alpha^2 R\,\mathrm{e}^{-2\mathrm{i}\epsilon t} \int_0^t [3\tilde{\rho}_{23}(s) - 2\tilde{\rho}_{12}(s)]\,\mathrm{d}s, \tag{74}$$

$$\dot{\tilde{\rho}}_{33}(t) = -2\alpha^2 R \int_0^t \cos[2\epsilon(t-s)][\tilde{\rho}_{33}(s) - \tilde{\rho}_{22}(s)]\,\mathrm{d}s, \tag{75}$$

$$\dot{\tilde{\rho}}_{14}(t) = -\alpha^2 R\,\mathrm{e}^{2\mathrm{i}\epsilon t} \int_0^t \mathrm{e}^{-\mathrm{i}(\epsilon-\kappa)s}\tilde{\rho}_{14}(s)\,\mathrm{d}s, \tag{76}$$

$$\dot{\tilde{\rho}}_{24}(t) = -2\alpha^2 R\,\mathrm{e}^{-2\mathrm{i}\epsilon t} \int_0^t \mathrm{e}^{\mathrm{i}(\epsilon+\kappa)s}\tilde{\rho}_{24}(s)\,\mathrm{d}s, \tag{77}$$

$$\dot{\tilde{\rho}}_{34}(t) = -\alpha^2 R\,\mathrm{e}^{2\mathrm{i}\epsilon t} \int_0^t \mathrm{e}^{-\mathrm{i}(\epsilon-\kappa)s}\tilde{\rho}_{34}(s)\,\mathrm{d}s, \tag{78}$$

$$\dot{\tilde{\rho}}_{44}(t) = 0, \tag{79}$$

where the correlation function is given by $R = \mathrm{tr}_B\{\frac{J_+J_-}{N}\rho_B(0)\} = \mathrm{tr}_B\{\frac{J_-J_+}{N}\rho_B(0)\}$. In the limit $N \to \infty$, we find that $R = \frac{2}{4+g\beta}$. Clearly, $\dot{\tilde{\rho}}_{11}(t) + \dot{\tilde{\rho}}_{22}(t) + \dot{\tilde{\rho}}_{33}(t) = 0$, as it should be because $\tilde{\rho}_{44}(t) = \rho_{44}(t) = \rho_{44}(0)$. The time-local master equation can be obtained by replacing the matrix elements $\tilde{\rho}_{ij}(s)$ in equations (70)–(79) by $\tilde{\rho}_{ij}(t)$. The integration of the resulting first-order differential equations yields solutions involving the exponential function. For example when $\epsilon = 0$, we find that

$$\rho_{13}(t) = \rho_{13}(0)\exp\left[-\frac{2\alpha^2 t^2}{4+g\beta}\right]. \tag{80}$$

This solution is valid only at short intervals of time; it quickly diverges from the exact solution as t increases. Nevertheless, we can see that the Gaussian behaviour is clearly reproduced.

4. Decoherence and entanglement evolution

From equation (39), we can see that the maximally entangled state $|0, 0\rangle$ does not evolve in time. The corresponding one-dimensional subspace $\mathbb{C}^1$ is thus decoherence free. Taking into account the unitarity condition of the time evolution operator $\mathbf{U}(t)\mathbf{U}^\dagger(t) = \mathbb{I}_4$, we find that the state $\frac{1}{3}\mathbb{I}_3$ is also decoherence free. Hence, the decoherence-free subspace of our model is of dimension 2. The qubits prepared in any linear combination of the above states do not perceive the surrounding environment. In contrast, any other pure state decoheres evolving into mixed one and hence loses partially or completely its purity.

Generally speaking, the elements of the reduced density matrix show partial decoherence. Indeed, by virtue of equations (63)–(65), it can be shown that the elements of the stationary density matrix $\rho(\infty)$ are given by

$$\rho_{11}(\infty) = \rho_{33}(\infty) = \frac{1}{8}\big[(3+\Sigma)\big(\rho_{11}^0 + \rho_{33}^0\big) + 2\rho_{22}^0(1-\Sigma)\big], \tag{81}$$

$$\rho_{12}(\infty) = \rho_{23}(\infty) = \frac{\rho_{12}^0 + \rho_{23}^0}{4}(1-\Sigma), \tag{82}$$

$$\frac{\rho_{13}(\infty)}{\rho_{13}^0} = \frac{3+\Sigma}{8}, \tag{83}$$

$$\frac{\rho_{14}(\infty)}{\rho_{14}^0} = \frac{\rho_{34}(\infty)}{\rho_{34}^0} = \frac{1}{2}\,\mathrm{e}^{-\mathrm{i}(\epsilon+\kappa)t}, \tag{84}$$

$$\rho_{22}(\infty) = \frac{1}{4}\big[(1-\Sigma)\big(\rho_{11}^0 + \rho_{33}^0\big) + 2\rho_{22}^0\Sigma\big], \tag{85}$$

$$\rho_{24}(\infty) = 0, \tag{86}$$

$$\rho_{44}(\infty) = \rho_{44}^0, \tag{87}$$

where $\Sigma = \frac{\epsilon^2}{4}(4+g\beta)\exp\big[\frac{\epsilon^2}{4}(4+g\beta)\big]\Gamma\big[0, \frac{\epsilon^2}{4}(4+g\beta)\big]$. Note that the latter quantity satisfies $0 \leqslant \Sigma \leqslant 1$. This allows us to find upper bounds of the asymptotic values of the matrix elements $\rho_{ij}(t)$. For instance, if $2\rho_{22}^0 \leqslant \rho_{11}^0 + \rho_{33}^0$ then we have $\rho_{11}(\infty) \leqslant \frac{1}{2}\big(\rho_{11}^0 + \rho_{33}^0\big)$ and $\rho_{13}(\infty) \leqslant \frac{1}{2}\rho_{13}^0$. Similarly, when $2\rho_{22}^0 \geqslant \rho_{11}^0 + \rho_{33}^0$ then $\rho_{11}(\infty) \leqslant \frac{1}{8}\big[2\rho_{22}^0 + 3\big(\rho_{11}^0 + \rho_{33}^0\big)\big]$, and $\rho_{22}(\infty) \leqslant \frac{1}{2}\rho_{22}^0$. The matrix elements $\rho_{14}(\infty)$ and $\rho_{34}(\infty)$ oscillate around half of their initial values with period equal to $2\pi/(\epsilon+\kappa)$. When $\epsilon = 0$, the asymptotic state is independent of the bath temperature.

4.1. Measures of decoherence and entanglement

Due to the decoherence process, initially pure states evolve into mixed ones. Thus it is natural to use the extent of mixing as a measure of decoherence. This task can be carried out with the help of the quantity

$$D(t) = 1 - \mathrm{tr}[\rho(t)^2], \tag{88}$$

usually called linear entropy or idempotency. The above measure is effectively a monotonic decreasing function of the purity of the system; it vanishes for pure states and reaches its maximum value, $D_{\max} = \frac{3}{4}$, for the completely mixed state $\frac{1}{4}\mathbb{I}_4$.

Although the linear entropy quantifies the decoherence, it does not provide any other information about the state of the system. The so-called *fidelity*, which we denote by $F(t)$, is a measure of decoherence that quantifies the deviation from the free evolution of the system, i.e. in the absence of the surrounding environment [33]. Explicitly, we have

$$F(t) = \mathrm{tr}[\bar{\rho}(t)\rho(t)], \tag{89}$$

where $\bar{\rho}(t)$ describes the evolution, under the influence of the Hamiltonian operator H_0, of the central system initially prepared in the pure state $\rho(0)$, namely

$$\bar{\rho}(t) = \mathrm{e}^{-\mathrm{i}H_0 t}\rho(0)\,\mathrm{e}^{\mathrm{i}H_0 t}, \qquad \mathrm{e}^{-\mathrm{i}H_0 t} = \begin{pmatrix} \mathrm{e}^{-\mathrm{i}\epsilon t} & 0 & 0 & 0 \\ 0 & \mathrm{e}^{\mathrm{i}\epsilon t} & 0 & 0 \\ 0 & 0 & \mathrm{e}^{-\mathrm{i}\epsilon t} & 0 \\ 0 & 0 & 0 & \mathrm{e}^{\mathrm{i}\kappa t} \end{pmatrix}. \tag{90}$$

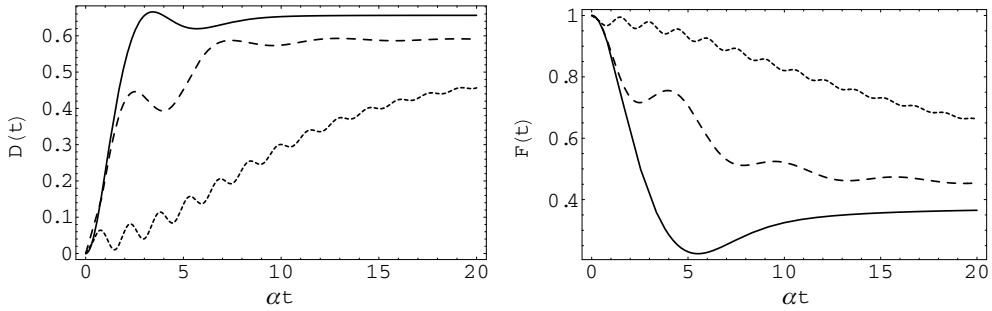

Figure 3. Time evolution of the linear entropy and the fidelity in the case of the initial state $|- -\rangle$ for different values of ϵ: $\epsilon = 0$ (solid lines), $\epsilon = 0.5\alpha$ (dashed lines) and $\epsilon = 2\alpha$ (dotted lines) with $g\beta = 10$.

Note that the fidelity reaches its maximum value $F_{\max} = 1$ if and only if $\rho(t) = \tilde{\rho}(t)$. Clearly, in the case of initial pure state $\rho(0) = |\Psi(0)\rangle\langle\Psi(0)|$, where $|\Psi(0)\rangle$ is an eigenvector of H_0, we simply have $\bar{\rho}(t) \equiv \rho(0)$. This means that the maximum values of the fidelity indicate the revival of the initial state when the latter is an eigenvector of H_0. We shall use this property when studying entanglement evolution.

In this work, we use the concurrence as a measure of entanglement between the central qubits. Recall that the concurrence corresponding to the reduced density matrix $\rho(t)$ is defined as [34]

$$C(\rho) = \max\{\sqrt{\lambda_1} - \sqrt{\lambda_2} - \sqrt{\lambda_3} - \sqrt{\lambda_4}, 0\} \tag{91}$$

where $\lambda_1, \lambda_2, \lambda_3$ and λ_4 are the eigenvalues, in descending order, of the operator

$$\varrho(t) = \rho(t)(\sigma_y \otimes \sigma_y)\rho^*(t)(\sigma_y \otimes \sigma_y) \tag{92}$$

written in $\mathbb{C}^2 \otimes \mathbb{C}^2$ and $\rho^*(t)$ designates the complex conjugate of the density matrix. The values of the concurrence range from zero, for unentangled states, to one for maximally entangled states. Since the concurrence is invariant under unitary transformations, we can rewrite the operator $\varrho(t)$ in the basis of the space $\mathbb{C}^3 \oplus \mathbb{C}^1$ as

$$\varrho(t) = \rho(t)V\rho^*(t)V, \qquad V = \begin{pmatrix} 0 & 0 & 1 & 0 \\ 0 & -1 & 0 & 0 \\ 1 & 0 & 0 & 0 \\ 0 & 0 & 0 & 1 \end{pmatrix}. \tag{93}$$

Below, we investigate decoherence and entanglement dynamics for some particular initial states that are of interest for applications. Other states can be studied with exactly the same method.

4.2. Results and discussion

Case 1: $|\Psi(0)\rangle = |\mp\mp\rangle$. Let us suppose that the tow-qubit system is initially prepared in the product state $|- -\rangle = |1, -1\rangle$. The corresponding time-dependent density matrix is diagonal; the idempotency is then equal to $D(t) = 1 - \sum_i [\rho_{ii}(t)]^2$. Since $|- -\rangle$ is an eigenvector of the Hamiltonian H_0, the fidelity simplifies to $F(t) = \rho_{11}(t)$. The time dependence of the linear entropy is shown in figures 3 and 4 for different values of the interaction strength ϵ and the bath temperature T. We can see that $D(t)$ increases starting from its initial value, zero, tending asymptotically to $D(\infty)$ which can be evaluated as $(21 - 2\Sigma - 3\Sigma^2)/32$. This

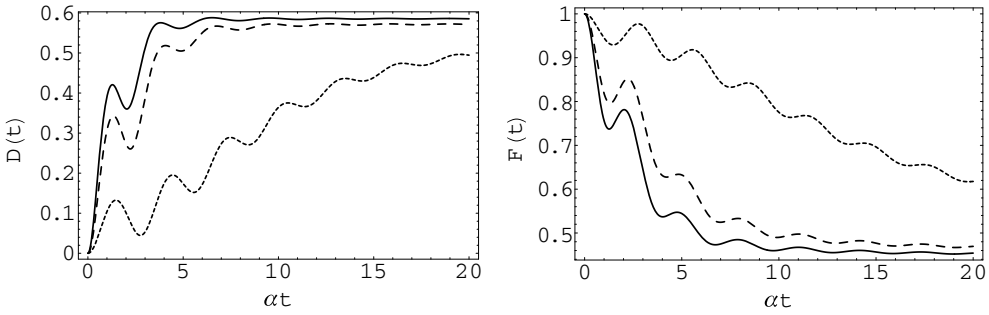

Figure 4. Time evolution of the linear entropy and the fidelity in the case of the initial state $|- -\rangle$ at different values of $g\beta$: $g\beta = 0$ (solid lines), $g\beta = 2$ (dashed lines) and $g\beta = 20$ (dotted lines) with $\epsilon = \alpha$.

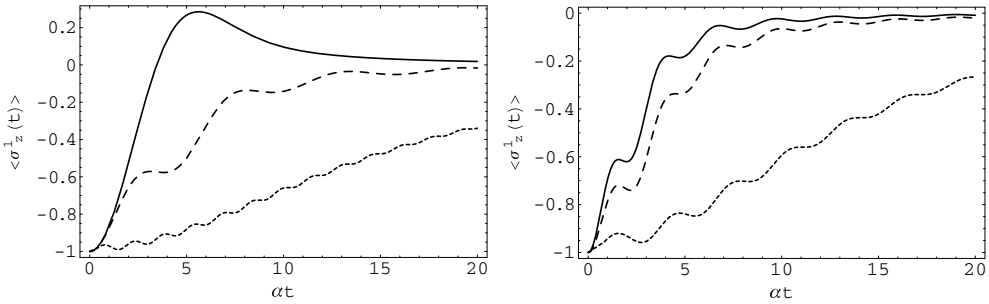

Figure 5. $\langle\sigma_z^1(t)\rangle$ versus the scaled time αt for different values of ϵ and $g\beta$: (i) $\epsilon = 0$ (solid lines), $\epsilon = 0.5\alpha$ (dashed lines) and $\epsilon = 2\alpha$ (dotted lines) with $g\beta = 10$ for the figure on the left; (ii) $g\beta = 0$ (solid lines), $g\beta = 2$ (dashed lines) and $g\beta = 20$ (dotted lines) with $\epsilon = \alpha$ for the figure on the right. The initial state is $|- -\rangle$.

limit assumes larger values as the strength of interactions ϵ decreases, in contrast, with the bath temperature T. Therefore, in order to ensure lower linear entropy, and consequently to reduce the effect of the environment, one has to increase (decrease) the value of the ratio ϵ/α (temperature T). Thus, we set $\Sigma = 1$ to find that $D_{\min}(\infty) = 0.5$. The fidelity shown in the above figures displays reverse behaviour compared to that of $D(t)$; its asymptotic value turns out to be $(3 + \Sigma)/8$ from which it follows that $F_{\max}(\infty) = 0.5$. It is quiet interesting to note that $D_{\min}(\infty) + F_{\max}(\infty) = 1$.

The mean value of the operator $\sigma_z^1(t) = 2S_z^1(t)$ corresponding to the first spin is found to be

$$\left\langle\sigma_z^1(t)\right\rangle = -[\cos(\epsilon t)\, f(t) + \sin(\epsilon t)\ell(t)]. \tag{94}$$

The latter quantity decays to zero, as shown in figure 5, indicating that the asymptotic state of the qubit is a fully mixture of the eigenvectors $|\pm\rangle$. Moreover, we can see that $\left\langle\sigma_z^1(t)\right\rangle$ decays slower at low bath temperatures and large values of ϵ. A straightforward calculation yields the following expression of the concurrence

$$C(t) = \max\{0, 2\max[\sqrt{\rho_{11}(t)\rho_{33}(t)}, \rho_{22}(t)] - 2\sqrt{\rho_{11}(t)\rho_{33}(t)} - \rho_{22}(t)\}. \tag{95}$$

It turns out that $C(t) \equiv 0$ independently of the values of ϵ and the temperature T. This implies that the state of the system is always separable; neither the interaction between the central

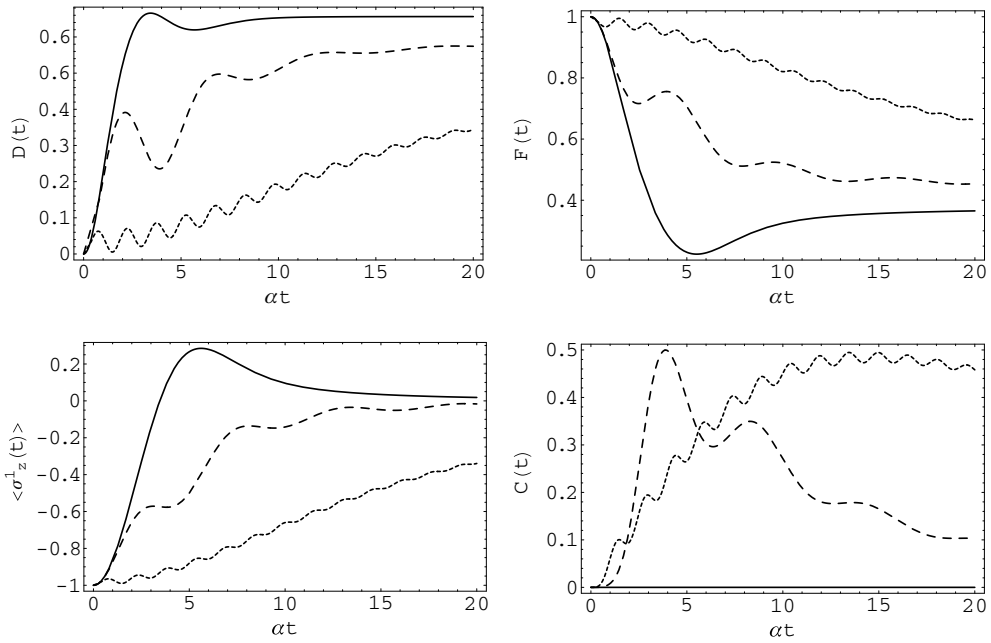

Figure 6. Time dependence of $D(t)$, $F(t)$, $\langle\sigma_z^1(t)\rangle$ and $C(t)$ for different values of λ in the case of the initial state $|-+\rangle$: $\lambda = 0$ (solid lines), $\lambda = 0.5\alpha$ (dashed lines) and $\lambda = 2\alpha$ (dotted lines) with $\Omega = 0$ and $g\beta = 10$.

qubits nor the coupling with the bath is able to generate entanglement. All the above results apply for the state $|++\rangle$ as well.

Case 2: $|\Psi(0)\rangle = |-+\rangle$. The state $|-+\rangle$ can be written as a combination of the states $|1,0\rangle$ and $|0,0\rangle$, namely $|-+\rangle = \frac{1}{\sqrt{2}}(|1,0\rangle + |0,0\rangle)$. In this case, the diagonal elements together with $\rho_{24}(t)$ are the only non-zero elements of the reduced density matrix. The idempotency, the fidelity and the mean value of $\sigma_z^1(t)$ are explicitly given by

$$D(t) = \tfrac{3}{4} - [\rho_{11}(t)]^2 - [\rho_{22}(t)]^2 - [\rho_{33}(t)]^2 - 2|\rho_{24}(t)|^2, \tag{96}$$

$$F(t) = \tfrac{1}{4}\{1 + 2\rho_{22}(t) + 4\,\mathrm{Re}[\rho_{24}(t)\,\mathrm{e}^{4i\Omega t}]\}, \qquad \left\langle\sigma_z^1(t)\right\rangle = -2\,\mathrm{Re}[\rho_{24}]. \tag{97}$$

The time dependence of the latter quantities is similar to that of the above case. When $\Omega = 0$, the asymptotic values of the linear entropy and the fidelity are, respectively, equal to $(21 - 2\Sigma - 3\Sigma^2)/32$ and $(3 + \Sigma)/8$. Hence we find again that $D_{\min}(\infty) = F_{\max}(\infty) = 0.5$ and $\lim_{t\to\infty}\langle\sigma_z^1(t)\rangle = 0$.

The expression of the concurrence is quiet long; we will not show it here for shortness. Nevertheless, we can distinguish to different cases. The first one corresponds to $\Omega = 0$, the variation in time of the corresponding concurrence is displayed in figures 6 and 7 for different values of λ and T. We can see that entanglement between the central qubits is generated when $\lambda \neq 0$ even though the initial state is separable. If there is no interaction between the central spins, the concurrence is always zero. We can see that the increase and the decay of the concurrence are faster at high temperatures and vice versa. Moreover, the numerical simulation shows that the concurrence never exceeds the value $C_{\max} = 0.5$: no

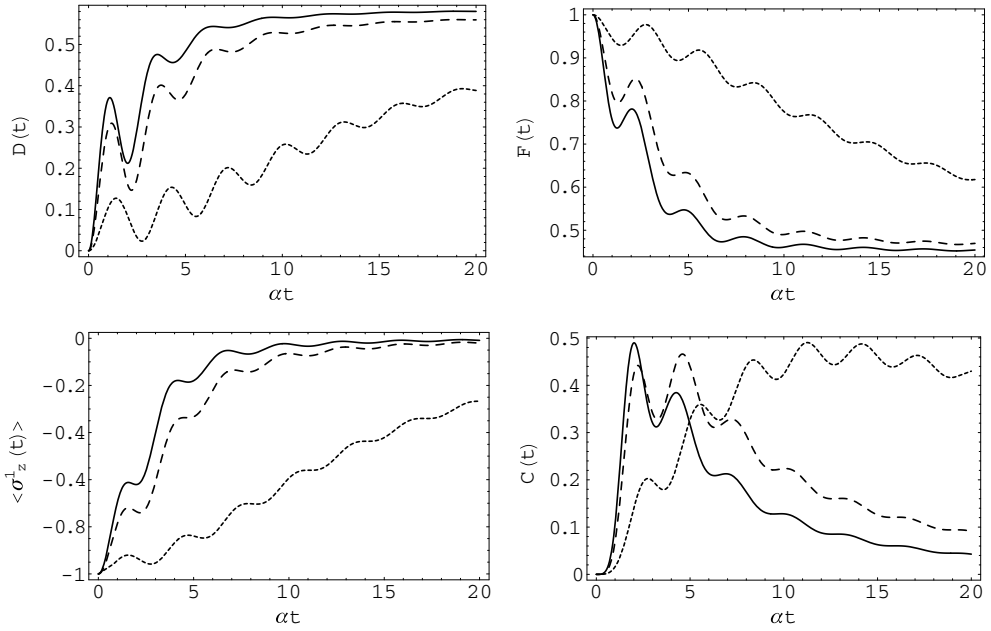

Figure 7. Evolution in time of $D(t)$, $F(t)$, $\langle\sigma_z^1(t)\rangle$ and $C(t)$ at different values of $g\beta$ in the case of the initial state $|-+\rangle$: $g\beta = 0$ (solid lines), $g\beta = 2$ (dashed lines) and $g\beta = 20$ (dotted line) with $\lambda = \alpha$ and $\Omega = 0$.

maximally entangled states can be produced in this case. Note that $|-+\rangle$ is an eigenvector of the Hamiltonian H_0, in the absence of the surrounding environment, the latter state remains always separable. Roughly speaking, the interaction with the spin bath changes the state of the central system so that the action of H_0 produces, to some extent, entanglement between the qubits.

The second case corresponds to $\Omega \neq 0$. Here $|-+\rangle$ is not an eigenvector of H_0; the action of the latter on this state periodically generates maximally entangled states. Hence, the effect of the environment consists of reducing the amount of the produced entanglement as shown in figure 8 . We can also see that the maximum values of $C(t)$ occur at moments of time for which $\langle\sigma_z^1(t)\rangle$ is equal to zero.

Case 3: $|\Psi(0)\rangle = \frac{1}{2}(|-\rangle + |+\rangle)^{\otimes 2}$. In this case, it can be shown that

$$D(t) = 1 - [\rho_{22}(t)]^2 - 2\{[\rho_{11}(t)]^2 + |\rho_{12}(t)|^2 + |\rho_{13}(t)|^2 + |\rho_{23}(t)|^2\}, \tag{98}$$

$$F(t) = \tfrac{1}{4}\{1 + \rho_{22}(t) + 2\,\mathrm{Re}[\rho_{13}(t)] + \sqrt{2}[(\rho_{12}^*(t) + \rho_{23}(t))\,\mathrm{e}^{-2\mathrm{i}\epsilon t} + \mathrm{c.c}]\}, \tag{99}$$

$$\langle\sigma_z^1(t)\rangle = 0. \tag{100}$$

Hence, the asymptotic value of the linear entropy is equal to $(267 + 114\Sigma^2 - 77\Sigma)/256$, from which it follows that $D_{\min}(\infty) = 19/32$. The dependence of $D(t)$ and $F(t)$ on ϵ is shown in figure 9; their variation with respect to T is quiet similar to that of the above two cases. The asymptotic fidelity shows periodic oscillations, its maximum value cannot be exactly determined. Since H_0 induces entanglement between the central qubits, we conclude that the influence of the environment consists of reducing the degree of entanglement of the central

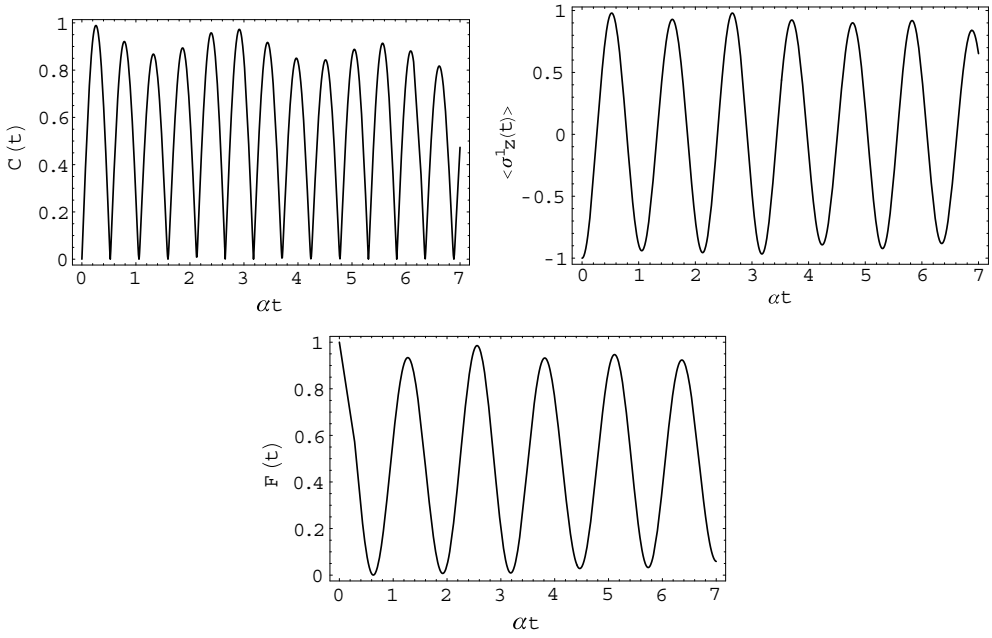

Figure 8. Time dependence of $C(t)$, $\langle\sigma_z^1(t)\rangle$ and $F(t)$ in the case of the initial state $|-+\rangle$ for $\lambda = 2\alpha$, $\Omega = \alpha$ and $g\beta = 10$.

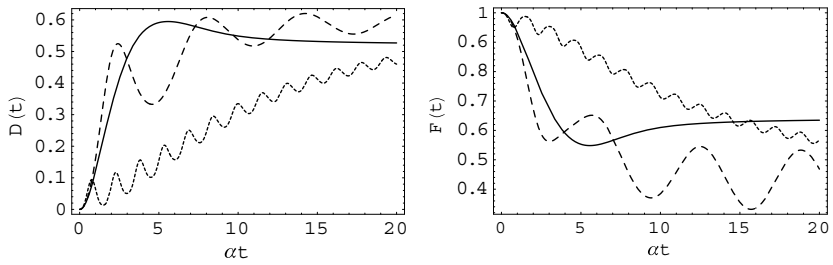

Figure 9. Time dependence of $D(t)$ and $F(t)$ at different values of ϵ in the case of the initial state $\frac{1}{2}(|-\rangle + |+\rangle)^{\otimes 2}$: $\epsilon = 0$ (solid lines), $\epsilon = 0.5\alpha$ (dashed lines) and $\epsilon = 2\alpha$ (dotted lines) with $g\beta = 10$.

system. This is shown in figure 10 where we have displayed the dynamics of entanglement at different values of ϵ.

Case 4: $|\Psi(0)\rangle = \frac{1}{\sqrt{2}}(|-+\rangle + |+-\rangle)$. If the initial state of the qubits is the maximally entangled state $|1,0\rangle$ then the density matrix is again diagonal. Since $|1,0\rangle$ is an eigenvector of H_0, we simply get $F(t) = \rho_{22}(t)$. The mean value of $\sigma_z^1(t)$ remains always zero. The behaviour of the linear entropy and the fidelity is shown in figures 11 and 12. The asymptotic values of the above measures are given by $(5 - 2\Sigma - 3\Sigma^2)/8$ and $(1 + \Sigma)/2$, respectively. Hence, we find that $D_{\min}(\infty) = 0$ and $F_{\max}(\infty) = 1$. Note that the above values are obtained for $\epsilon, \beta \to \infty$. This implies that the state of the qubits can be protected from decohering at very low bath temperatures or when their mutual interactions are sufficiently strong.

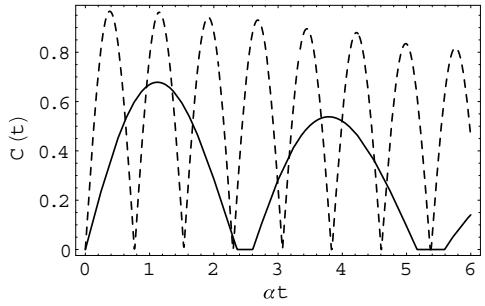

Figure 10. $C(t)$ versus αt at different values of ϵ in the case of the initial state $\frac{1}{2}(|-\rangle + |+\rangle)^{\otimes 2}$: $\epsilon = 0.5$ (solid line), $\epsilon = 2\alpha$ (dashed line) with $g\beta = 10$. The concurrence corresponding to $\epsilon = 0$ is identically zero.

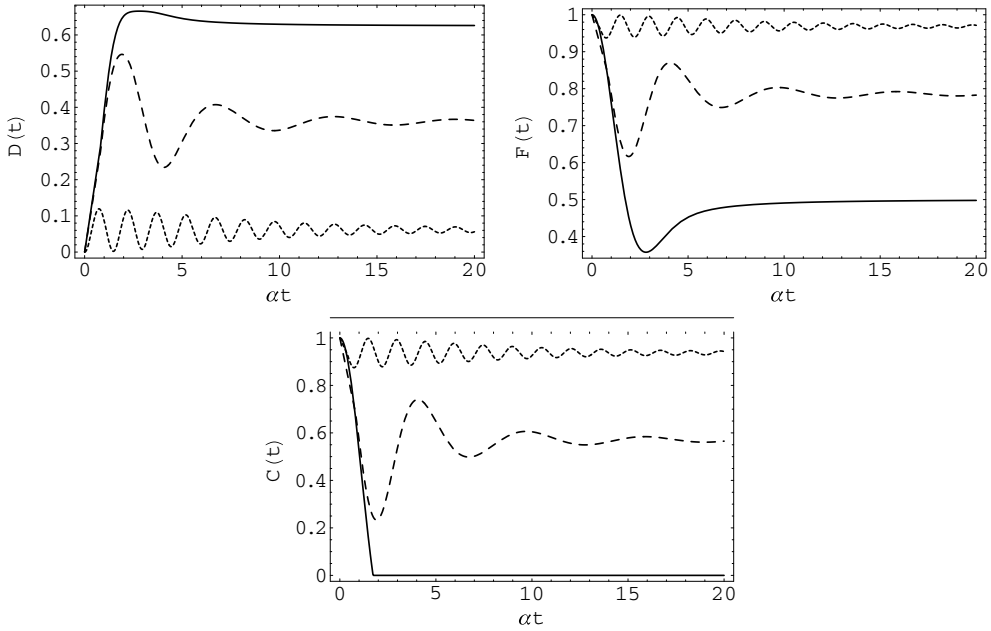

Figure 11. Time dependence of $D(t)$, $F(t)$ and $C(t)$ at different values of ϵ in the case of the maximally entangled state $\frac{1}{\sqrt{2}}(|- +\rangle + |+ -\rangle)$: $\epsilon = 0$ (solid lines), $\epsilon = 0.5\alpha$ (dashed lines) and $\epsilon = 2\alpha$ (dotted lines) with $g\beta = 10$.

The concurrence in this case is given by relation (95). We can see from figure 11 that for $\epsilon = 0$ the concurrence decays from its maximum value to vanish at a certain value of time, the state of the two-qubit system becomes separable. This behaviour is known as the entanglement sudden death which has been investigated for bosonic environments [35]. As we increase the value of the interaction strength ϵ, the concurrence approaches its initial maximum value $C_{\max} = 1$. This happens when the fidelity, in turn, approaches its maximum value implying that the initial state of the two-qubit system revives. For example, the asymptotic value of the concurrence turns out to be

$$C(\infty) = \Sigma. \tag{101}$$

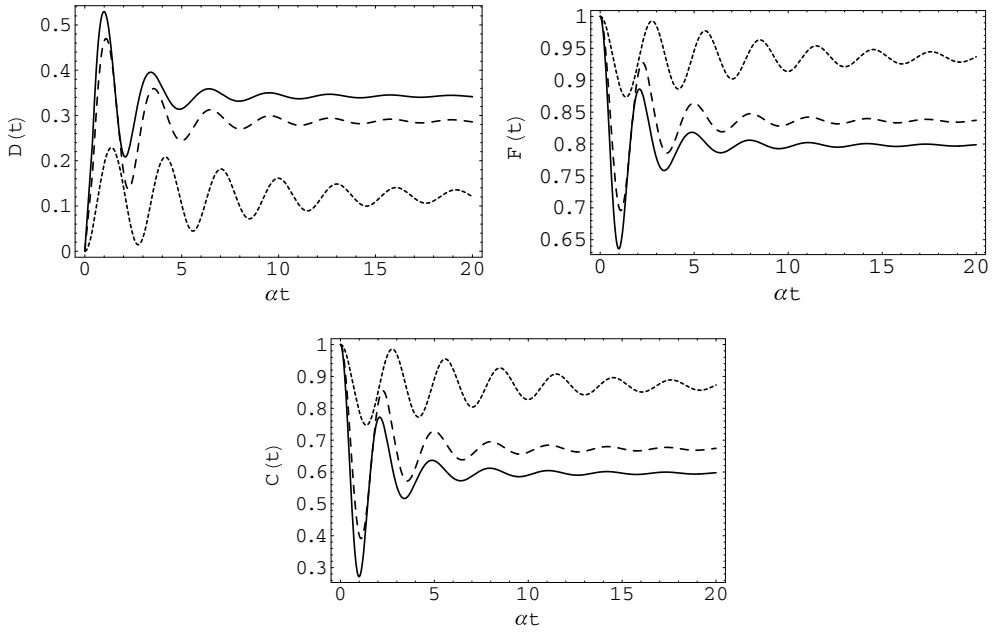

Figure 12. Variation in time of $D(t)$, $F(t)$ and $C(t)$ for different values of $g\beta$ in the case of the maximally entangled state $\frac{1}{\sqrt{2}}(|-+\rangle + |+-\rangle)$: $g\beta = 0$ (solid lines), $g\beta = 2$ (dashed lines) and $g\beta = 20$ (dotted lines) with $\epsilon = \alpha$.

Since the quantity Σ is a monotonic increasing function of both ϵ and β, and satisfies $\lim_{\epsilon,\beta\to\infty}\Sigma = 1$, we simply obtain $C_{\max}(\infty) = F_{\max}(\infty) = 1$. When $\epsilon \neq 0$ the concurrence may vanish for a certain interval of time then revives again to tend to its asymptotic value (101). If ϵ is sufficiently large, the concurrence never vanishes as displayed in figure 11.

Case 5: $|\Psi(0)\rangle = \frac{1}{\sqrt{2}}(|++\rangle + |--\rangle)$. In this case, the non-zero elements of the reduced density matrix are $\rho_{11}(t)$, $\rho_{22}(t)$, $\rho_{33}(t)$ and $\rho_{13}(t)$. Consequently, the mean value of $\sigma_z^1(t)$ remains always zero. The idempotency and the fidelity are given by

$$D(t) = 1 - 2([\rho_{11}(t)]^2 + [\rho_{13}(t)]^2) - [\rho_{22}(t)]^2, \qquad F(t) = \rho_{11}(t) + \rho_{13}(t). \tag{102}$$

The asymptotic values of the above measures are, respectively, given by $(75 - 14\Sigma - 13\Sigma^2)/128$ and $(9 + 3\Sigma)/16$. It follows that $D_{\min}(\infty) = 0.375$ and $F_{\max}(\infty) = 0.75$

The square roots of the eigenvalues of the matrix $\varrho(t)$ can be easily calculated; they are given explicitly by $\rho_{22}(t)$, $|\rho_{11}(t) + \rho_{13}(t)|$ and $|\rho_{11}(t) - \rho_{13}(t)|$. Hence, the concurrence in this case is given by

$$C(t) = \max\{0, 2\max[\rho_{22}(t), |\rho_{11}(t) + \rho_{13}(t)|, |\rho_{11}(t) - \rho_{13}(t)|] - \rho_{22}(t) - |\rho_{11}(t) + \rho_{13}(t)| - |\rho_{11}(t) - \rho_{13}(t)|\}. \tag{103}$$

From figure 13, we can see that even when $\epsilon = 0$ the asymptotic value of the concurrence is different from zero. Indeed, by a direct calculation we find

$$C(\infty) = \frac{1 + 3\Sigma}{8}, \tag{104}$$

implying that $0.125 \leqslant C(\infty) \leqslant 0.5$. By contrast with $|1, 0\rangle$, the maximally entangled state $\frac{1}{\sqrt{2}}(|1, -1\rangle + |1, 1\rangle)$ does not revive, its entanglement cannot be recovered even for large

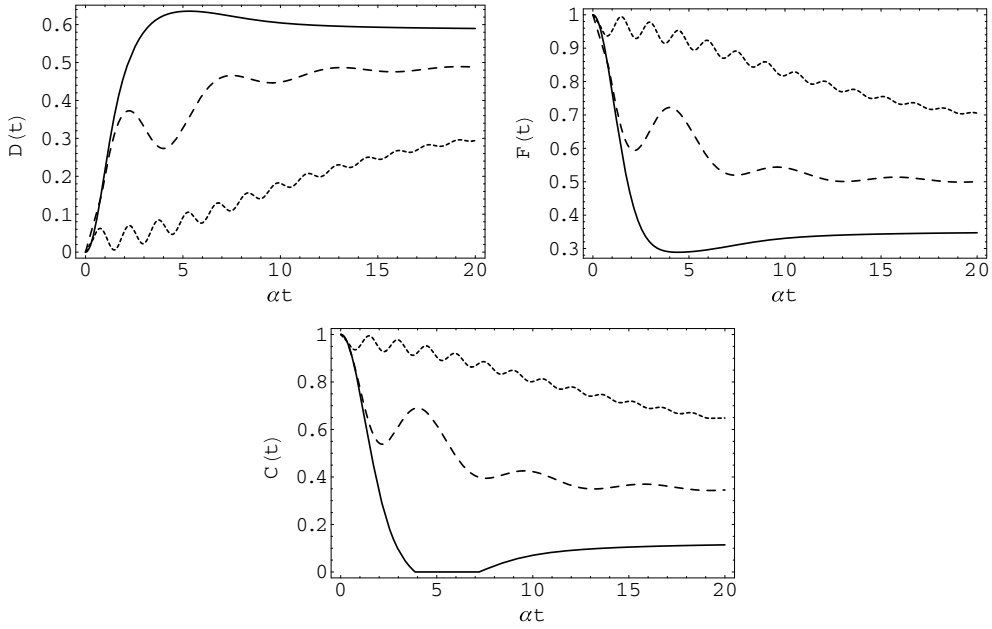

Figure 13. Time dependence of $D(t)$, $F(t)$ and $C(t)$ at different values of ϵ in the case of the maximally entangled state $\frac{1}{\sqrt{2}}(|- -\rangle + |++\rangle)$: $\epsilon = 0$ (solid lines), $\epsilon = 0.5\alpha$ (dashed lines) and $\epsilon = 2\alpha$ (dotted lines) with $g\beta = 10$.

values of ϵ at very low temperatures of the bath. We also see that for noninteracting qubits, entanglement vanishes for some interval (dark period) then revives again.

Case 6: Werner states. Let us consider Werner states

$$\rho_W^0 = \tfrac{1}{4}(1-p)\mathbb{I}_4 + p|\Phi\rangle\langle\Phi|, \tag{105}$$

where $|\Phi\rangle = \frac{1}{\sqrt{2}}(|- -\rangle + |++\rangle)$ and $0 \leqslant p \leqslant 1$. In $\mathbb{C}^3 \oplus \mathbb{C}^1$ the above density matrix takes the form

$$\rho_W^0 = \begin{pmatrix} \frac{1+p}{4} & 0 & \frac{p}{2} & 0 \\ 0 & \frac{1-p}{4} & 0 & 0 \\ \frac{p}{2} & 0 & \frac{1+p}{4} & 0 \\ 0 & 0 & 0 & \frac{1-p}{4} \end{pmatrix}. \tag{106}$$

The corresponding stationary density matrix is then equal to

$$\rho_W^\infty = \begin{pmatrix} \frac{2+p(1+\Sigma)}{8} & 0 & \frac{p(3+\Sigma)}{16} & 0 \\ 0 & \frac{1-p\Sigma}{4} & 0 & 0 \\ \frac{p(3+\Sigma)}{16} & 0 & \frac{2+p(1+\Sigma)}{8} & 0 \\ 0 & 0 & 0 & \frac{1-p}{4} \end{pmatrix}. \tag{107}$$

The maximum values of the asymptotic linear entropy and fidelity are, respectively, given by $(6-3p^2)/8$ and $(1+2p^2)/4$. The largest eigenvalue of the operator ϱ^∞ is equal to

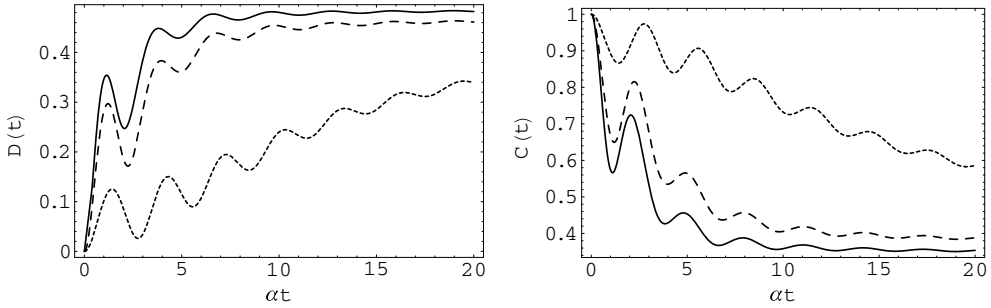

Figure 14. Variation in time of $D(t)$ and $C(t)$ for different values of $g\beta$ in the case of the maximally entangled state $\frac{1}{\sqrt{2}}(|- -\rangle + |++\rangle)$: $g\beta = 0$ (solid lines), $g\beta = 2$ (dashed lines) and $g\beta = 20$ (dotted lines) with $\epsilon = \alpha$.

$(4 + 5p + 3p\Sigma)/16$, the remaining ones read $(1 - p)/4$, $(1 - p\Sigma)/4$ and $(4 + p\Sigma - p)/16$. The asymptotic value of the concurrence is then equal to

$$C(\rho_W^{\infty}) = \max\left\{0, \frac{1}{8}[p(3\Sigma + 5) - 4]\right\}. \tag{108}$$

Therefore, the two-qubit system is entangled if and only if

$$p > \frac{4}{5 + 3\Sigma}. \tag{109}$$

The minimum value of p for which the asymptotic state of the qubits is entangled is equal to 0.5 which corresponds to $\epsilon \to \infty$ and/or $T \to 0$. The behaviour of the concurrence in this case is similar to that of $|\Phi\rangle$.

To conclude our discussion we note that in [36], the fidelity of any mixed state, calculated with respect to a maximally entangled state, is shown to be bounded above by $[1 + C(t)]/2$. This fully agrees with our results as can be seen in the case of the maximally entangled state $|1, 0\rangle$. Indeed, when $\rho_{22}(t) \geqslant \rho_{11}(t)$ then $C(t) = \max[2\rho_{22}(t) - 1, 0] = \max[2F(t) - 1, 0]$. The corresponding asymptotic values do satisfy the latter condition. The above equality implies that the concurrence is equal to the negativity [36]. The critical point at which $C(t)$ vanishes corresponds to $F(t) = 0.5$ (see figure 11). These results also hold for $C(t)$ and $F(t)$ corresponding to the state $\frac{1}{\sqrt{2}}(|++\rangle + |- -\rangle)$ at least at long times. In [37], numerical simulation was used to study entanglement dynamics of two qubits coupled to the anisotropic bath. The authors found that concurrence can be produced in the case of the initial states $|\pm\pm\rangle$, if the qubits are subjected to an external magnetic field. It would then be interesting to investigate this situation analytically.

5. Conclusion

In conclusion we have studied decoherence and entanglement dynamics of two qubits interacting with the antiferromagnetic spin bath at thermal equilibrium. The time evolution operator of the composite system was analytically derived using symmetry properties of the model Hamiltonian. The reduced density matrix was calculated by performing the partial trace over the irrelevant bath degrees of freedom. In the limit of an infinite number of spins in the environment, N, the lowering and raising operators corresponding to the total angular momentum, as well as its z-component, converge to normal random variables. This enabled

us to calculate the partial trace when $N \to \infty$. The above limit turns out to be a very good approximation for finite numbers of spins. We found that the off-diagonal elements of the reduced density matrix show partial decoherence. The decoherence-free subspace in this model is spanned by the states $|0,0\rangle\langle 0,0|$ and $\frac{1}{3}\mathbb{I}_3$. Using the linear entropy and the fidelity, we studied decoherence of the central qubits for different initial states. We showed that the decay of the elements of the reduced density matrix is Gaussian, which is a hallmark of non-Markovian dynamics. The effect of decoherence can be reduced at a low bath temperature and strong coupling between the central qubits.

Entanglement behaviour depends on the initial states of the qubits. The concurrence remains always zero when the central qubits are initially prepared in the pure product states $|\pm\pm\rangle$. These remain always separable. In contrast, the qubits become entangled if they are prepared in the states $|\pm\mp\rangle$ or $\frac{1}{2}(|-\rangle+|+\rangle)^{\otimes 2}$. In the latter case, the entanglement generation is due to mutual interactions between the central qubits. The situation is different in the case of the states $|\pm\mp\rangle$ which are the eigenvectors of the free Hamiltonian when $\Omega = 0$: this is an example of environment-induced entanglement. Initially entangled states lose partially or completely their entanglement. This behaviour strongly depends on the bath temperature and the strength of interactions between qubits. It is found that entanglement can be protected to some extent from decohering at low bath temperatures and/or strong interactions between the central qubits if they are prepared in the maximally entangled state $|1,0\rangle$. For small values of ϵ, it is found that entanglement displays sudden death. Finally, I think that the results presented here help extending the class of exactly solvable models for spin systems.

Acknowledgments

The author acknowledges the financial support from the South African National Research Foundation. This work was partially carried out during the visit of YH to Institut de Physique, Université Mentouri-Constantine, Algeria.

References

[1] Einstein A, Podolsky B and Rosen N 1935 *Phys. Rev.* **47** 777
[2] Schrödinger E 1935 *Naturwissenschaften* **23** 807
[3] Bell J S 1964 *Physics* **1** 195
[4] Nielsen M A and Chuang I L 2000 *Quantum Computation and Quantum Information* (Cambridge: Cambridge University Press)
[5] Bennett C H and Wiesner S J 1993 *Phys. Rev. Lett.* **69** 2881
[6] Bennett C H and DiVincenzo D P 2000 *Nature* **404** 247
[7] Bennett C H, Brassard G, Crépeau C, Jozsa R, Peres A and Wootters W K 1993 *Phys. Rev. Lett.* **70** 1895
[8] Bennett C H, DiVincenzo D P, Smolin J A and Wootters W K 1996 *Phys. Rev.* A **54** 3824
[9] Lloyd S 1993 *Science* **261** 1569
[10] Ekert A and Josza R 1998 *Philos. Trans. R. Soc. Lond.* A **356** 1769
[11] Loss D and DiVincenzo D P 1998 *Phys. Rev.* A **57** 120
[12] Burkard G, Loss D and DiVincenzo D P 1999 *Phys. Rev.* B **59** 2070
[13] Zurek W H 1991 *Phys. Today* **44** 36
[14] DiVincenzo D P and Loss D 2000 *J. Magn. Magn. Mater.* **200** 202
[15] Zurek W H 2003 *Rev. Mod. Phys.* **75** 715–75
[16] Shor P W 1995 *Phys. Rev.* A **52** R2493
[17] Preskill J 1998 *Proc. R. Soc. Lond.* A **454** 385
[18] Reina J H, Quiroga L and Johnson N F 2002 *Phys. Rev.* A **65** 032326
[19] Gottesman D 1996 *Phys. Rev.* A **54** 1862
[20] Steane A M 1996 *Phys. Rev. Lett.* **77** 793
[21] Lidar D A, Chuang I L and Whaley K B 1998 *Phys. Rev. Lett.* **81** 2594

[22] Lidar D A, Bacon D and Whaley K B 1999 *Phys. Rev. Lett.* **82** 4556
[23] Prokof'ev N V and Stamp P C E 2000 *Rep. Prog. Phys.* **63** 669
[24] Hamdouni Y, Fannes M and Petruccione F 2006 *Phys. Rev.* B **73** 245323
[25] Yuan X Z, Goan H J and Zhu K D 2007 *Phys. Rev.* B **75** 045331
[26] Huang Z, Sadiek G and Kais S 2006 *J. Chem. Phys.* **124** 144513
[27] Breuer H P, Burgarth D and Petruccione F 2004 *Phys. Rev.* B **70** 045323
[28] Bhaktavatsala Rao D D, Ravishankar V and Subrahmanyam V 2006 *Phys. Rev.* A **74** 022301
[29] Hamdouni Y and Petruccione F 2007 submitted
[30] Von Waldenfels W 1990 *Séminaire de probabilité (Starsburg)* tome 24 (Berlin: Springer) pp 349–56
[31] Wang X and Mølmer K 2002 *Eur. Phys. J.* D **18** 385
[32] Danos M and Rafelski J 1984 *Pocketbook of Mathematical Functions* (Frankfurt: Verlag Harri Deutsch)
[33] Fedichkin L and Privman V 2006 v2 *Preprint* cond-mat/0610756
[34] Wootters W K 1998 *Phys. Rev. Lett.* **80** 2245
[35] Yu T and Eberly J H 2004 *Phys. Rev. Lett.* **93** 140404
[36] Verstraete F and Verschelde H 2002 *Phys. Rev.* A **66** 022307
[37] Jing J and LÜ Z 2007 *Phys. Rev.* B **75** 174425